Soil-structure interaction effects on modal analysis of a 3D reticulated structure supporting plane rectangular shells

Lucas P. de Souza[1], Patrick de O. B. da Costa[1], Dhionata W. M. Santos[1], Daniel C. de M. Candido[1], Paulo de O. Weinhardt[1]

[1]*Flextronics Institute of Technology*
Av. Liberdade, 6615, Building 4, 18087-170, Sorocaba/São Paulo, Brazil
lucas.desouza@fit-tecnologia.org.br, patrick.batista@fit-tecnologia.org.br, daniel.candido@fit-tecnologia.org.br

Abstract. This paper aims to verify the interference of soil-structure interaction (SSI) on the natural frequencies and on the respective vibration modes of a 3D reticulated structure supporting plane rectangular shells. This is done through a computational linear elastic 3D finite element model using Euler-Bernoulli frame elements, biquadratic Lagrangian thin shell elements and elastic translation springs for the soil at columns bases (representing pile embedded length). A convergence analysis is performed to determine the maximum mesh size and mass participation factors are measured to establish the number of considered vibration modes. Chosen elastic spring coefficients are extracted using polynomial linear regression applied to the results of experimental compressive and horizontal load tests of steel piles embedded in a silty clay soil. Using these parameters, nine models are processed via an eigen solver and obtained frequencies and some mode shapes are presented. It is found that, for the adopted approach and for the evaluated structure, there are not significant changes in modal response induced by SSI, being the mass distribution more important than soil stiffness in this case. Despite the results, this study indicates the need of further investigation to provide better measures about the interference of SSI on modal response of structures as the one analyzed in this research.

Keywords: Finite Element analysis, Modal analysis, Soil-structure dynamic interaction

1 Introduction

Modal analysis can be performed to estimate the dynamic properties such as the frequencies and vibration modes of the system. These modal characteristics are relevant for a better understanding of structural behavior under considerable static external loads, and especially with respect to dynamic excitation, e.g., wind and seismic loads. Nevertheless, in civil engineering, modal analysis is usually performed using finite element models and constituted in idealized form, i.e., undamped structures fixed at the base in order to disregard any interaction with the soil [1]. However, depending on the type of structure, results obtained considering the interaction with the soil may differ significantly from the response of the same structure when fully fixed [2, 3]. Wolf [4] and Papadopoulos et al. [5] emphasize that the effects of soil-structure interaction (SSI) should not be neglected as they can increase the flexibility of the structural system as well as its damping.

In this context, the objective of this paper is to perform a preliminary check on the influence of soil deformability on the modal response of a 3D reticulated structure supporting plane rectangular shells. This is done using a linear elastic 3D mixed frame-shell finite element model (implemented in Python 3 language [6]) and horizontal and vertical springs placed at columns bases, representative of piles embedded length. Compared modal results are natural frequencies and correspondent mode shapes. Besides, comments about mass modal participation and center of mass position are also included. In the end, some suggestions for additional studies are given.

2 Methodology

2.1 Geometry

In short, the analyzed structure is formed by plane rectangular shells fixed on a continuous longitudinal steel beam, which is in turn supported by vertical ground soil-based steel columns. Cited columns have part of its length

above the ground and the other part is embedded in the soil, behaving as a pile. However, the embedded length is not explicitly modeled: linear springs at ground surface are considered to reproduce the deformability of these elements. The origin of global coordinate system is placed at the left tip of longitudinal beam, being x-axis parallel to this component's axis. Vertical direction is parallel to z-global axis and y-axis is horizontal and orthogonal to x-axis. All these described features can be identified in figure 1. Due to the reticulated nature of the idealized model, geometry generation includes the calculation of master node positions of each component. Also, inertia-based vectors are determined for each structural part, orienting the cross-sectional weak axes with respect to global system.

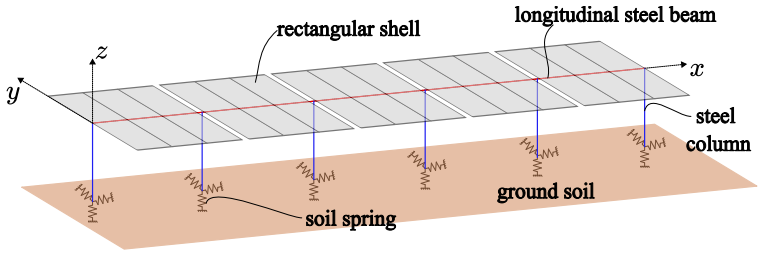

Figure 1. Geometry components and global axis positioning.

2.2 Mesh generation

Excepting shell surfaces, all structural components are modeled as Euler-Bernoulli elastic 3D frame elements, with 2 nodes per element and 6 DOFs per node - 3 translations and 3 rotations. Shells are discretized as 9-node bi-quadratic Lagrangian shells with 6 DOFs per node. Each snippet between two master nodes is subdivided into a discrete number of frame elements according to a pre-established maximum element length $l_{e_{\max}}$. For shell elements, edge nodes are taken from frame discretization and internal nodes are generated. Values of $l_{e_{\max}}$ equal to 0.80, 0.40, 0.20, 0.10 and 0.05 m are tested in order to find an optimized mesh size using the convergence criterion $c_{f_i} = \left[\sum_{n=1}^{n_{modes}} (\Delta f_n^i)^2\right] / \left[1 + \sum_{n=1}^{n_{modes}} (f_n^0)^2\right] \leq 5 \times 10^{-4}$, being n the current vibration mode, n_{modes} the number of vibration modes, i the index of current mesh size, $\Delta f_n^i = f_n^i - f_n^{i-1}$ the frequency variation between two consecutive mesh sizes, f_n^i the frequency of n-th mode calculated using the i-th mesh size and f_n^0 the frequencies calculated using the coarser mesh size ($l_{e_{\max}} = 0.80$ m). After analyzing this convergence factor, it is concluded that $l_{e_{\max}} = 0.10$ m is enough to provide accurate results, as shown in figure 2. This value is used for all models in this paper.

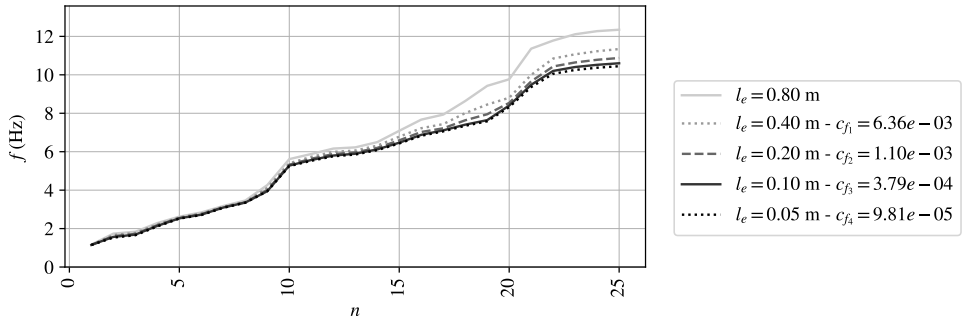

Figure 2. Convergence analysis as a function of mesh refinement for FIXED9 model.

2.3 Soil deformability approach

There are several manners of modeling pile-soil system and the complexity can vary considerably. Some possible approaches are dynamic Winkler foundation, analytical elastic-column formulations, boundary element method and dynamic finite-element models [7]. In this article, soil behavior is idealized as linear springs attached to the columns base at ground surface level, disregarding pile embedded length. Subgrade reaction moduli are estimated using experimental results obtained from horizontal and compressive load tests of steel driven piles in

a silty clay soil. In these tests, the pile/column is tested under compression - by a vertical (z-axis) quasi-static load applied to top end - and under horizontal lateral load - parallel to y-axis (major-axis is resisting). Produced displacements are measured close to the ground surface level (above) and load-displacement curves are determined in vertical and horizontal directions of the pile/column.

As shown in figures 3, both vertical and major-axis horizontal spring elastic coefficients (reaction moduli) are estimated as the derivatives of polynomial curves fitted to load test point cloud data. For the compression case, these values are taken at displacements equal to 0.75 (STIFF models) and 1.50 mm (SOFT models). Horizontal springs in major axis (y-axis) direction have elastic coefficients calculated when displacements are equal to 12.50 (STIFF models) and 25.00 mm (SOFT models). Elastic coefficients in minor-axis (x-axis) direction are adopted as 1.5 times that ones calculated for the major-axis.

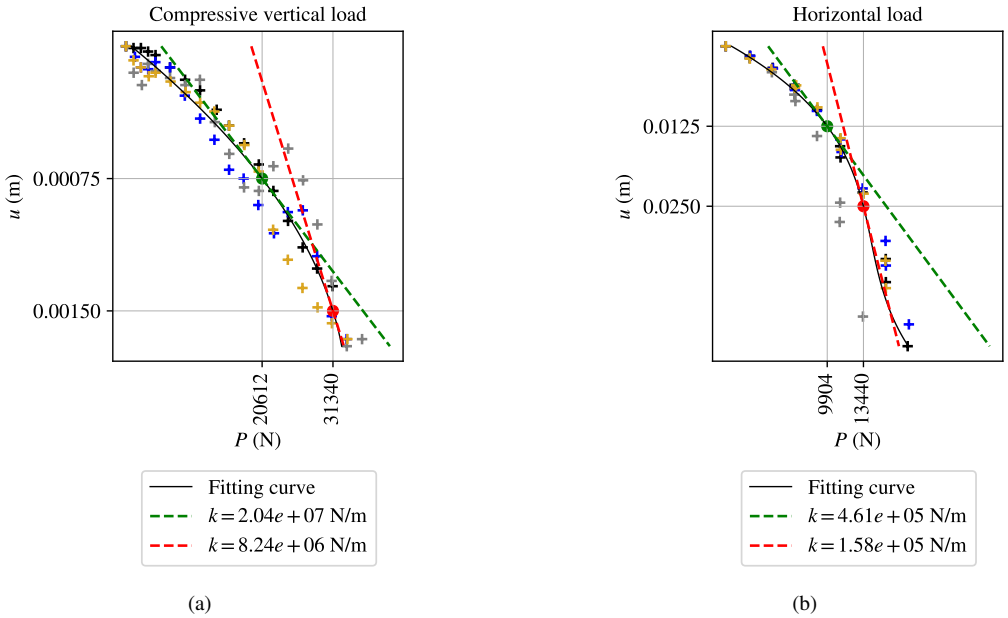

Figure 3. Calculation of soil elastic coefficients in (a) vertical (z-axis) and (b) horizontal (y-axis) directions.

The adoption of two different stiffness levels is intended to simulate soil stiffness changes under different load levels. Also, soil is considered spatially homogeneous, so the reaction moduli are the same for all columns/piles. Soil damping is a property not contemplated in this study and this simplification is assumed based on statements as found in He & Fu [8], declaring that the presence of damping does not change every aspect of modal analysis of undamped systems. This purpose is made for this specific work as an introduction to the theme, although more robust assumptions could be required for deeper studies.

2.4 Modal analysis parameters

Lumped mass matrix formulation was considered for the analyses and all kinds of damping are ignored. Also, the eigen problem is solved using ARPACK (Implicitly Restarted Arnoldi Methods) solver [9]. The number of analyzed vibration modes, in turn, was chosen based on the following criterion: once the predominant excitation applied to this structure is parallel to y-axis translation DOF, the amount of modes must be sufficient to accumulate more than 95% of mass participation in this direction; additionally, all modes with more than 1% of individual mass participation (with respect to any DOF) are considered. It is in accordance with EN 1998-1 [10] code, which states that the sum of the effective modal masses for the modes taken into account needs to be at least 90% of the total mass of the structure and that all modes with effective modal masses greater than 5% of the total mass have to be assessed. The adopted strategy, when applied to FIXED9 model, leads to the consideration of 25 vibration modes as shown in figure 4.

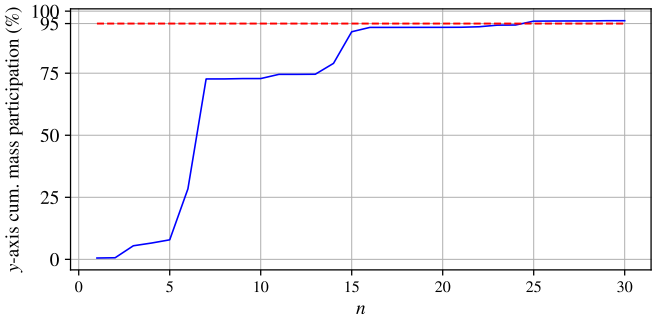

Figure 4. Cumulative percentage mass participation factors in y-axis direction for FIXED9 model.

2.5 Analyzed models

Analyzed models are listed in table 1 and illustrated in figure 5, all of them presenting 4 internal spans (with 3, 6 or 9 rectangular shells per span) followed by a cantilever span with 3 shells (this parameter does not change among models). Also, soil deformability is considered by varying spring coefficients (reaction moduli) at columns base nodes according to what is defined in 2.3.

Table 1. Analyzed models

model	k_x (N/m)	k_y (N/m)	k_z (N/m)	rect. shells per span	length (m)	mass (kg)
FIXED3	-	-	-	3	19.65	1021.12
STIFF3	6.92×10^5	4.61×10^5	2.04×10^7	3	19.65	1021.1
SOFT3	2.37×10^5	1.58×10^5	8.24×10^6	3	19.65	1021.1
FIXED6	-	-	-	6	34.29	1718.88
STIFF6	6.92×10^5	4.61×10^5	2.04×10^7	6	34.29	1718.88
SOFT6	2.37×10^5	1.58×10^5	8.24×10^6	6	34.29	1718.88
FIXED9	-	-	-	9	48.93	2416.64
STIFF9	6.92×10^5	4.61×10^5	2.04×10^7	9	48.93	2416.64
SOFT9	2.37×10^5	1.58×10^5	8.24×10^6	9	48.93	2416.64

3 Results and discussions

Natural frequencies obtained from analyses of all models are presented in table 2. For the applied soil approach and specifically for the considered silty clay soil, frequency results do not change substantially with the the consideration of soil deformability at columns ground base. When taking SSI approach into account, all frequencies tend to slightly increase with respect to fully fixed models. STIFF3 and SOFT3 model frequencies, for instance, show the highest difference against FIXED3 frequencies (+0.057 %) for the 4^{th} vibration mode, a structural oscillation in longitudinal direction - x-axis translation of longitudinal steel beam, according to figure 6.

Models STIFF6 and SOFT6, in turn, have the major difference in natural frequencies for the 3^{rd} mode, with an increase of +0.034% in relation to FIXED6 model. This mode shape is also a x-axis translation of longitudinal beam and is displayed in figure 7. A similar phenomenon is detected in results of STIFF9 and SOFT9 models, for which highest frequency difference concerning the FIXED9 frequencies (+0.032%) occur in the 5^{th} mode of figure 8.

Even being small frequency differences, the fact of highest changes have occurred for longitudinal x-axis

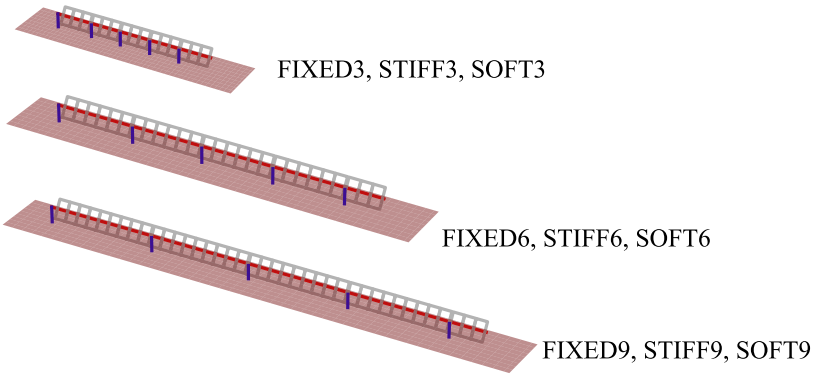

Figure 5. Geometry of analyzed models.

Table 2. Natural frequencies for FIXED3, FIXED6, and FIXED9 models (Hz).

mode	FIXED3	STIFF3	SOFT3	FIXED6	STIFF6	SOFT6	FIXED9	STIFF9	SOFT9
1	2.526	2.526	2.526	1.621	1.621	1.621	1.149	1.149	1.149
2	2.737	2.737	2.737	2.186	2.186	2.186	1.568	1.568	1.568
3	4.015	4.015	4.015	2.741	2.742	2.742	1.686	1.686	1.686
4	4.057	4.059	4.059	3.612	3.613	3.613	2.141	2.141	2.141
5	7.008	7.008	7.008	3.875	3.875	3.875	2.533	2.534	2.534
6	7.586	7.586	7.586	4.116	4.116	4.116	2.725	2.725	2.725
7	7.796	7.796	7.796	4.554	4.554	4.554	3.095	3.095	3.095
8	8.667	8.667	8.667	4.682	4.682	4.682	3.354	3.354	3.354
9	9.914	9.914	9.914	4.812	4.812	4.812	3.947	3.947	3.947
10	10.179	10.179	10.179	7.080	7.080	7.080	5.277	5.277	5.277

translation probably is due to imposed constraints: only the first steel column supports longitudinal steel beam translation and other columns allow x-axis frictionless sliding. It means there is just one vertical element and just one foundation restricting this movement.

Concerning the slight frequency increment after inputting soil deformability, the center of mass position is moved down in vertical direction (negative z-axis), when fixed nodes at columns bases are substituted by elastic springs (fixed masses are switched to moving masses). Since the soil reaction modulus is high enough, the structural mass lever arm with respect to the ground becomes the governing parameter, resulting in higher frequencies of STIFF and SOFT models when compared with FIXED ones.

The natural frequency results obtained for STIFF and SOFT models are exactly the same for adopted soil stiffness values, regardless of the structure longitudinal length and total mass. Even reducing horizontal springs elastic stiffness by 65.73% and vertical springs elastic stiffness by 59.61% frequencies remain the same. This behavior is equal for mass modal participation factors, also the same for STIFF and SOFT models. A possible reason for these results is that, for flexible structures like the ones studied herein, mass distribution along FE nodes is much more important than stiffness distribution along these nodes. Therefore, high changes in stiffness matrices - as the imposition of soil deformability - tend to keep results of FIXED models. Great part of obtained modal responses depend on rectangular shell masses, which are the most flexible and heavy structural components.

Considering the scope of this study, presented results show that, given a choice between either ignoring or including below grade SSI, imposing a fixed boundary condition at grade level would be representative. Although, it does not mean that soil deformability have no influence on the structural dynamic response. For a time-history analysis conclusions could be different. Even for modal analysis, more complex soil behavior could be incorporated to the study for better conclusions, what includes distributed springs along pile embedded length. In accordance with Kavitha, Beena and Narayanan [11], a softer soil consistency causes an increase in the pile fixity depth, decreasing the natural frequency of the referred system.

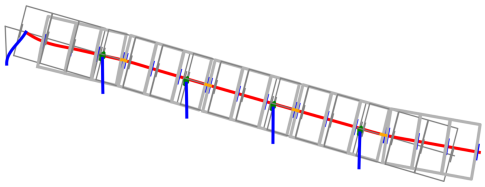

Figure 6. 4^{th} vibration mode of SOFT3 model.

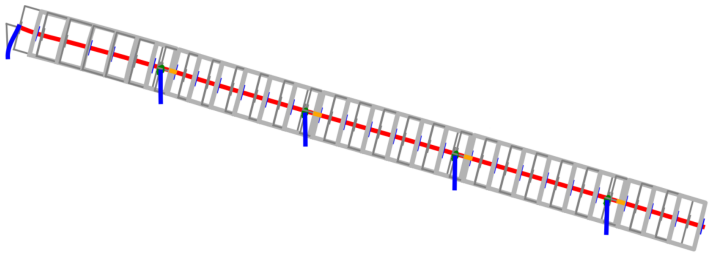

Figure 7. 3^{rd} vibration mode of SOFT6 model.

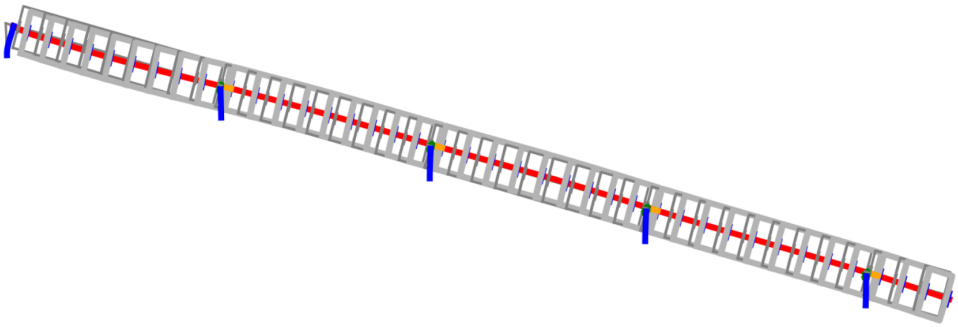

Figure 8. 5^{th} vibration mode of SOFT9 model.

Also, there were not measured any effect of SSI supports on the structural damping or incorporated any soil damping property to the model, something that could affect the response when a damped modal analysis is considered. A correlated example is found in Bao et al. [12], where the structural damping ratios are extracted from field experimental tests and then incorporated to the computational analysis. Additionally, 3D solid finite elements could be accounted for a most representative analysis.

4 Final remarks

In this study, a preliminary analysis of SSI effects on the modal response of a 3D reticulated structure supporting plane rectangular shells is conducted. A general assembly is adopted, with rectangular shells fixed on a longitudinal steel beam supported by steel columns. Euler-Bernoulli 3D frame elements are used to represent all reticulated components, bi-quadratic Lagrangian thin shells simulate surface components (rectangular shells) and elastic spring elements represent soil behavior. The optimal maximum mesh size $l_{e_{\max}} = 0.10$ m is determined after a convergence analysis through a quadratic convergence criterion. For soil deformability approach, experimental data from load tests performed for a silty clay soil is used. In this procedure, polynomial curves are adjusted via linear regression to fit displacement-load point cloud values and spring elastic stiffness is taken as the derivatives of referred fitting functions. Furthermore, the number of evaluated vibration modes (25) is established by examining individual and cumulative percentage modal mass participation in each one of 6 existing DOFs.

In this context, 6 different models are processed, varying among them the ground soil boundary conditions and the number of rectangular shells per span. Obtained results show that, for the considered situations, vibration frequencies do not present significant changes with and without elastic supports. For chosen structural configurations, mass distribution along the components seems to be more important than soil stiffness. Against expectations, natural frequencies of models with elastic supports are slightly higher than those ones calculated for fully fixed

supports. There is still no consensus about the influence of SSI in structural dynamic response. Then, further studies must be done and possible improvements are springs distributed along pile embedded length, account of soil damping or soil as 3D solid finite elements and dynamic behavior under forced vibration considering SSI.

Acknowledgements

The authors acknowledge the support of Flextronics Institute of Technology (FIT).

References

[1] M. Lou, H. Wang, X. Chen, and Y. Zhai. Structure–soil–structure interaction: Literature review. *Soil dynamics and earthquake engineering*, vol. 31, n. 12, pp. 1724–1731, 2011.
[2] J. Bielak. Modal analysis for building-soil interaction. *Journal of the Engineering Mechanics Division*, vol. 102, n. 5, pp. 771–786, 1976.
[3] B. Manna and D. K. Baidya. Nonlinear dynamic response of piles under horizontal excitation. *Journal of Geotechnical and Geoenvironmental Engineering*, vol. 136, n. 12, pp. 1600–1609, 2010.
[4] J. Wolf. *Dynamic soil-structure-interaction Englewood Cliffs*. Prentice Hall, 1985.
[5] M. Papadopoulos, R. Van Beeumen, S. François, G. Degrande, and G. Lombaert. Computing the modal characteristics of structures considering soil-structure interaction effects. *Procedia engineering*, vol. 199, pp. 2414–2419, 2017.
[6] G. Van Rossum and F. L. Drake. *Python 3 Reference Manual*. CreateSpace, Scotts Valley, CA, 2009.
[7] K. Kuo and H. Hunt. Dynamic models of piled foundations. *Applied Mechanics Reviews*, vol. 65, 2013.
[8] Z. Fu and J. He. *Modal Analysis*. Elsevier Science, 2001.
[9] D. C. S. R. B. Lehoucr and C. Yang. Arpack users' guide: Solution of large scale eigenvalue problems with implicitly restarted arnoldi methods, 1997.
[10] Europeean Comitee for Standardisation. *Design of structures for earthquake resistance – Part 1: General rules, seismic actions and rules for buildings*. Brussels, 2004.
[11] B. K. S. P. E.. Kavitha and K. P. Narayanan. A review on soil–structure interaction analysis of laterally loaded piles. *Innovative Infrastructure Solutions*, vol. 14, 2016.
[12] T. Bao, Z. Li, O. Pu, R. W. Chan, Z. Zhao, Y. Pan, Y. Yang, B. Huang, and H. Wu. Modal analysis of tracking photovoltaic support system. *Solar Energy*, vol. 265, pp. 112088, 2023.